

Precise peculiar velocities from gravitational waves accompanied by electromagnetic signals and cosmological applications

Y. Y. Wang¹, F. Y. Wang^{1,2*} and Y. C. Zou^{3†}

¹*School of Astronomy and Space Science,
Nanjing University, Nanjing 210093, China*

²*Key Laboratory of Modern Astronomy and Astrophysics (Nanjing University),
Ministry of Education, Nanjing 210093, China*

³*School of Physics,
Huazhong University of Science and Technology,
Wuhan 430074, China*

**Electronic address: fayinwang@nju.edu.cn*

†Electronic address: zouyc@hust.edu.cn

(Dated: October 3, 2021)

Peculiar velocities are a precious tool to study the large-scale distribution of matter in the local universe and test cosmological models. However, present measurements of peculiar velocities are based on empirical distance indicators, which introduce large error bars. Here we present a new method to measure the peculiar velocities, by directly estimating luminosity distances through waveform signals from inspiralling compact binaries and measuring redshifts from electromagnetic (EM) counterparts. In the future, with the distance uncertainty of GW events reducing to 0.1 per cent by future GW detectors, the uncertainty of the peculiar velocity can be reduced to 10 km/s at 100 mega parsecs. We find that dozens of GW events with EM counterparts can provide a Hubble constant H_0 uncertainty of 0.5% and the growth rate of structure with a 0.6% precision in the third-generation ground-base GW detectors, which can reconcile the H_0 tension and determine the origins for cosmic accelerated expansion.

PACS numbers:

I. INTRODUCTION

Recently, the Advanced LIGO and Advanced Virgo discovered the first gravitational wave (GW) signal from coalescing binary neutron stars accompanied by electromagnetic (EM) counterparts[1–3]. This breakthrough heralds the new era of gravitational-wave multi-messenger astronomy. GW measurements of coalescing binaries can make cosmological measurements. Schutz first pointed out that the waveform signal from inspiralling compact binaries can be used to measure the luminosity distance to the source with high precision[4]. GW standard sirens can probe the cosmic expansion history and the dark energy with high accuracy[5, 6]. Similar to standard candles, an independent measure of the redshifts of EM counterparts is crucial. Mergers of binary neutron stars (BNSs) or neutron star-black hole (NS-BH) binaries are the most promising GW sources accompanied by detectable EM counterparts. The discovery of EM counterparts of GW170817 has realized this idea[2]. Therefore, GWs together with EM counterparts providing the redshift information, could be an excellent cosmological probe.

When using GWs and EM counterparts to measure the distance-redshift relation, the redshifts should be entirely due to the cosmic expansion. However, in the local universe, large-scale structure induces peculiar motions so that the measured redshifts contain contributions from peculiar velocities[7, 8]. Meanwhile, the horizon of Advanced LIGO and Advanced Virgo for the merger of BNS or NS-BH is only a few hundreds Mpc[9]. If we take the

typical value of peculiar velocity $v_{\text{pec}} = 400 \text{ km s}^{-1}$, and Hubble constant $H_0 = 70 \text{ km s}^{-1} \text{ Mpc}^{-1}$, the peculiar velocity can contribute about 30% of the measured redshift at a distance of 20 Mpc. Therefore, the effect of peculiar velocities on GW astronomy is crucial in local universe. Previous works using GW and EM counterparts as cosmological tool do not consider this effect. Meanwhile, peculiar velocities are important for directly probing the distribution of dark matter[7], studying precision cosmology from type Ia supernovae (SNe Ia)[10, 11], measuring the Hubble constant[12], probing the growth rate[13] and redshift space distortion[14, 15]. In consequence, measurement of peculiar velocity is of great importance for cosmology[16].

At present, there are two ways to measure peculiar velocities. The first method is to measure peculiar velocities directly by obtaining distances to individual galaxies and their redshifts. Therefore, the accuracy of peculiar velocities depends on distance indicators. Many distance indicators independent of Hubble constant have been used, including SNe Ia[17], Tully-Fisher relation[18–20] and the fundamental plane relation[21]. However, there are several sources of systematic error, such as Malmquist bias, luminosity evolution, and imperfect corrections for dust extinction for SNe Ia. At the same time, the Tully-Fisher relation and the fundamental plane relation yield individual distance uncertainties of 20%-25%[8, 22]. The second method measures the peculiar velocities statistically based on redshift space distortion[14]. Unfortunately, the peculiar velocities derived from both methods have large uncertainties[16].

Below, we calculate the peculiar velocity of the host galaxy of GW170817. By fitting the waveform signal of the GW170817, the distance of this event is $43.8^{+2.9}_{-6.9}$ Mpc[23]. From the EM counterparts, the heliocentric redshift of host galaxy NGC 4993 is $z = 0.009783$ [24], which corresponds to $z = 0.01083$ in the CMB frame. In order to derive the peculiar velocity from equation (1), the Hubble constant should be known. Recent measurement of the local Hubble constant from SNe Ia is claimed to be accurate at the 2.4% level[25], suggesting $H_0 = 73.24 \pm 1.74 \text{ km s}^{-1} \text{ Mpc}^{-1}$. However, this value is 3.4σ higher than $67.8 \pm 0.9 \text{ km s}^{-1} \text{ Mpc}^{-1}$ predicted by Λ CDM model from Planck cosmic microwave background (CMB) data[26]. The radial peculiar velocity is $v_{\text{pec},r} \simeq 276 \text{ km s}^{-1}$ if H_0 from Planck is used. Using the error propagation formula, the uncertainty of $v_{\text{pec},r}$ is about 200 km s^{-1} . The radial peculiar velocity turns out to be $v_{\text{pec},r} \simeq 38 \text{ km s}^{-1}$ for H_0 from SNe Ia[25]. So, the radial peculiar velocity is heavily dependent on the Hubble constant H_0 . In local universe, they degenerate with each other.

The peculiar velocity of NGC 4993 was also derived using a dark-matter simulation from the Constrained Local Universe Simulations project[27]. However, the initial conditions of peculiar velocities are derived from the Tully-Fisher relation and the fundamental plane relation[27]. By assuming a small error of recession velocity, the peculiar velocity with a small error is obtained. Abbott et al. (2017b)[23] used the 6dF galaxy redshift survey peculiar velocity map[28] to derive the peculiar velocity of NGC 4993. The uncertainties of peculiar velocities depend on the errors of distance and Hubble constant. Generally they are proportional to d_L . We compare peculiar velocities' uncertainties for different methods at a distance of 100 Mpc. With this distance, the errors of peculiar velocities from SNe[17] are in the range of $(500, 1000) \text{ km s}^{-1}$. From SFI++ data set[20], they are roughly $(800, 3000) \text{ km s}^{-1}$ at 100 Mpc from the galaxy survey with Tully-Fisher relation. These errors together with that of NGC 4993 (GW170817) are listed in figure 1 for comparison.

II. METHOD AND RESULTS

Here we propose a robust method to measure the peculiar velocities with high accuracy using GWs and EM counterparts. Based on the observed redshift z and the luminosity distance d_L derived from GW waveform signal, the radial peculiar velocity v_p can be calculated by

$$v_{\text{pec},r} = cz - H_0 d_L, \quad (1)$$

where c is the speed of light and H_0 is the Hubble constant. Because of the H_0 tension[41], we should provide an independently measured H_0 to calculate $v_{\text{pec},r}$. If H_0 is measured precisely in the future, $v_{\text{pec},r}$ can be derived directly from equation (1).

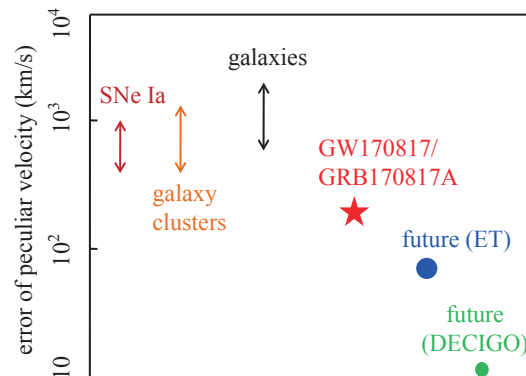


FIG. 1: Measurement accuracy of the peculiar velocity at 100 Mpc for different methods. The method with label ‘SNe Ia’ is from Riess et al. (1997) [17], with label ‘galaxy clusters’ is from Colless et al. (2001) [29], and with label ‘galaxies’ is from Springob et al. (2007) [20]. The error from our method is the star with label ‘GW170817/GRB170817A’. The future capable uncertainties of peculiar velocities are labelled as ‘future (ET)’ and ‘future (DECIGO)’.

Our method is called $v - v$ comparison method[17, 39, 40]. It is performed by comparing the radial peculiar velocities from GW observations with those reconstructed from the galaxy survey.

In the standard Λ CDM cosmology, gravitational instability induces the growth of density perturbations, which generate the peculiar velocity field. In the regime where the density perturbation is linear, the peculiar velocity (\vec{v}_{pec}) can be expressed as[7]

$$\vec{v}_{\text{pec}}(\vec{x}) = \frac{H_0 f_0}{4\pi} \int d^3 \vec{x}' \delta_{\text{m}}(\vec{x}', t_0) \frac{(\vec{x}' - \vec{x})}{|\vec{x}' - \vec{x}|^3}, \quad (2)$$

where f_0 is the present day growth rate of structure, and $\delta_{\text{m}} = (\rho - \bar{\rho})/\bar{\rho}$ is the dimensionless density contrast. The growth rate of structure at scale factor a is defined as

$$f(a) \equiv \frac{d \ln D(a)}{d \ln a} \quad (3)$$

where D is the linear growth factor[7].

It is common to assume that a linear bias exists between galaxy fluctuations δ_g and matter fluctuations δ_{m} by introducing the bias parameter b , i.e., $\delta_g = b\delta_{\text{m}}$. So the growth rate of density fluctuations f can be replaced with the parameter $\beta \equiv f/b$. The β can be combined with $\sigma_{8,g}$ to get the growth rate since $f\sigma_8 = \beta\sigma_{8,g}$.

Branchini et al. (1999) presents a self-consistent non-parametric model of the local peculiar velocity field derived from the distribution of IRAS galaxies in the Point Source Catalogue redshift (PSCz) survey[33]. The catalogue contains 15795 galaxies and the peculiar velocity field is reconstructed assuming $\beta = 1$. The true peculiar velocities are proportional to β . Since the value of β is

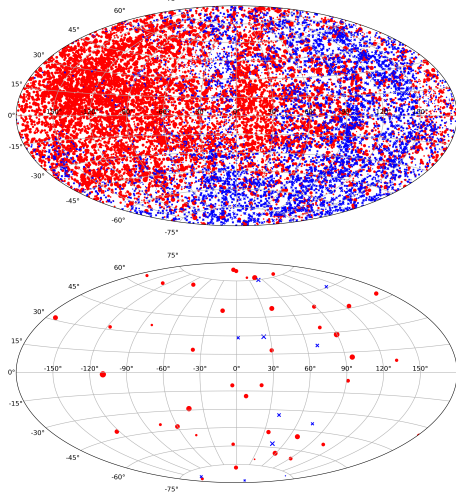


FIG. 2: Peculiar velocities of PSCz galaxies (15795 galaxies in total) and mock GW events projected in Galactic coordinates. Upper panel: the red circles and blue crosses represent PSCz galaxies that are moving away from and moving towards us, respectively. Lower panel: the same as upper panel but for mock GW events. The size of markers is proportional to the magnitude of the line-of-sight peculiar velocity in each panel. The value of $H_0 = 67.8 \text{ km s}^{-1} \text{ Mpc}^{-1}$ from Planck Collaboration is used.

uncertain, we need to constrain β and H_0 simultaneously by comparing the peculiar velocities from equation (3) with measured peculiar velocities. Galaxies in the PSCz redshift catalogue were used to trace the underlying mass density field within $300 h^{-1} \text{ Mpc}$ under the assumption of linear and deterministic bias[36]. Using the iterative technique[37], the model velocity field is obtained from the positions of galaxies in redshift space according to equation (2). In our calculation, we interpolate model velocities at the positions of mock GW events to compare predicted and observed velocities. The predicted velocities in GW location are calculated by applying a Gaussian kernel of radius R_j (5 Mpc in this paper) to the predicted 3D velocity $\mathbf{v}_{\text{rec}}(\mathbf{x}_j)$ specified at the position of the PSCz galaxies. We have

$$\mathbf{v}_{\text{smo}}(\mathbf{x}_i) = \frac{\sum_{j=1}^{N'} \mathbf{v}_{\text{rec}}(\mathbf{x}_j) \exp\left(-\frac{(\mathbf{x}_j - \mathbf{x}_i)^2}{2R_j^2}\right)}{\sum_{j=1}^{N'} \exp\left(-\frac{(\mathbf{x}_j - \mathbf{x}_i)^2}{2R_j^2}\right)}. \quad (4)$$

Then the predicted radial peculiar velocities are

$$v_{\text{model},i} = \mathbf{v}_{\text{smo}}(\mathbf{x}_i) \cdot \mathbf{x}_i. \quad (5)$$

We construct a mock GW catalogue to compare measured peculiar velocities with PSCz survey[33]. Abbott et al. (2016) estimated the detection rate of BNS coalescences to be 4-80 per year for Advanced LIGO and Advanced Virgo after 2020, which will increase to 11-180 per year after 2024 with more detectors[9]. Fortunately, the ET would observe $10^3 - 10^7$ BNS mergers per

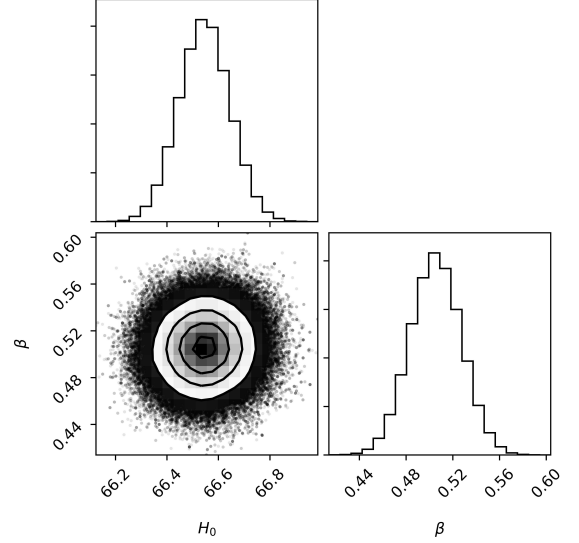


FIG. 3: Constraints on β and H_0 using $v - v$ comparison method from mock GW catalogue. Confidence contours (1σ , 2σ and 3σ) and marginalized likelihood distributions for the parameters (H_0, β) are shown. The error of distance derived from GW waveform fitting is assumed as 1%. Our method can constrain the Hubble constant and β simultaneously.

year[30]. For the third-generation ground-based GW detectors (such as ET), the precise localization and distance uncertainty from GW signals for BNSs could be sufficient to directly identify the host galaxies[34] at $z < 0.1$. Meanwhile, the proposed space-based GW detector Big Bang Observer (BBO)'s angular resolution would be sufficient to uniquely identify the host galaxy of compact binary merger[6]. Here we conservatively construct a mock GW catalog containing 90 events for the third-generation ground-based GW detector ET. The spatial positions of BNSs are randomly sampled in the sky and their volume density is uniform in the range $[0, 0.045]$, which is the farthest reach to 190 Mpc—the boundary of PSCz reconstructed peculiar velocity field[39]. The simulated heliocentric redshifts of GW host galaxies are transformed to CMB-frame redshifts by

$$1 + z_{\text{CMB}} = (1 + z_{\text{hel}}) \left[1 + \frac{v_{\text{CMB}}}{c} (\hat{\mathbf{n}}_{\text{CMB}} \cdot \hat{\mathbf{n}}) \right], \quad (6)$$

where $\hat{\mathbf{n}}$ is the direction cosine of GW source's sky position, $\hat{\mathbf{n}}_{\text{CMB}} = (263.99^\circ, 48.26^\circ)$ and $v_{\text{CMB}} = 369 \text{ km/s}$ [35]. The luminosity distance d_L is obtained by fitting GW waveform signal. In our simulation, they are generated from the redshift-distance relation of Planck15/ Λ CDM model[26] with normally distributed discrepancy. In figure 2, we show the radial peculiar velocities of PSCz galaxies[33] and our mock GW events projected in Galactic coordinates.

We employ python module `emcee`[38] to constrain H_0 and β simultaneously. The maximum likelihood estima-

tion (MLE) is applied to the MCMC algorithm. The likelihood L is the summation of many normal distributions

$$L = \prod_{i=1}^N \frac{1}{\sqrt{2\pi}\sigma_i} \exp \left[-\frac{(v_{\text{pec},r,i} - \beta v_{\text{model},i})^2}{2\sigma_{v_{\text{pec},r,i}}^2} \right], \quad (7)$$

where

$$v_{\text{pec},r,i} = cz_i - H_0 d_{L,i}, \quad (8)$$

and

$$\left(\frac{\sigma_{v_{\text{pec},r,i}}}{H_0 d_{L,i}} \right)^2 = \left(\frac{\sigma_{H_0}}{H_0} \right)^2 + \left(\frac{\sigma_{d_L}}{d_L} \right)^2. \quad (9)$$

For the third-generation detectors, such as Einstein Telescope (ET)[30], we adopt $\frac{\sigma_{H_0}}{H_0} \sim 1\%$ and $\frac{\sigma_{d_L}}{d_L} \sim 1\%$. Then the log-likelihood is

$$\ln L = -\frac{1}{2} \sum_{i=1}^N \left[\frac{-(v_{\text{pec},r,i} - \beta v_{\text{model},i})^2}{2\sigma_{v_{\text{pec},r,i}}^2} + \ln(2\pi\sigma_{v_{\text{pec},r,i}}^2) \right]. \quad (10)$$

The priors of H_0 and β are $[60, 80](\text{km s}^{-1} \text{Mpc}^{-1})$ and $[0, 1]$, respectively. Figure 3 shows the 1σ to 3σ confidence contours and marginalized likelihood distributions for $\{H_0, \beta\}$ from MCMC fitting. The constraints are $H_0 = 66.55 \pm 0.10 \text{ km s}^{-1} \text{Mpc}^{-1}$ (1σ) and $\beta = 0.504 \pm 0.022$ (1σ) respectively. The β value is consistent with those of previous works, but with a smaller uncertainty.

The ability of our method depends on the measurement accuracies of the Hubble constant H_0 and luminosity distance d_L . At present, the value of H_0 can be determined at 1% accuracy from CMB in the Λ CDM model[26]. For BNSs, the distance accuracy by Advanced LIGO can reach 10%. The main uncertainty comes from the errors of the distances measured by GW detectors. For the third-generation detectors, such as ground-based ET[30], space-based BBO[6] and Deci-Hertz Interferometer Gravitational wave Observatory (DECIGO)[31], the distance uncertainties could be as low as 1% [30] and 0.1% [6, 31] in local universe, respectively. In the future, the uncertainty of the H_0 can also be decreased to 0.1% [6, 32], together with the uncertainty of d_L decreased to 0.1%, the errors of peculiar velocities can be determined to $\sim 10 \text{ km/s}$ including the uncertainty of redshift determination at 100 Mpc. We also plot the errors of peculiar velocities measured by the future GW detectors in figure 1. From this figure, the future uncertainty of the peculiar velocity can be about one order of magnitude smaller than the current available uncertainties. On the other hand, once the inclination angle of the GW is determined by other independent method, the uncertainty of the distance can be reduced enormously, as the distance and the inclination angle degenerate.

Next we will discuss the cosmological applications of the precise peculiar velocities derived from our method. One well-known problem of standard Λ CDM model is

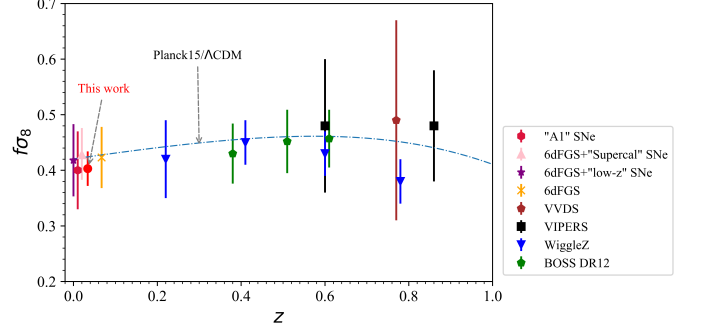


FIG. 4: Estimates of $f\sigma_8(z)$ for different methods. Our constraint is shown as the red data point. We also show past measurements of the $f\sigma_8(z)$ from 6dFGS at $z \simeq 0$ and SNe[45], SNe[46], 6dFGS and “Supercal” SNe[47], 6dFGS $z = 0.067$ [48], WiggleZ[49], VVDS[50], BOSS[51], and VIPERS[52]. The growth parameter $f\sigma_8(z)$ as function of z under Planck/ Λ CDM is calculated with python module CAMB[53], which is shown as dash-dotted line.

the tension between the relatively higher growth rate $f(z)\sigma_8(z)$ found in CMB experiments and the smaller one obtained from large-scale galaxy surveys[42]. Recent study shows that they are in 5σ tension with each other[43]. Using β constrained by our method, we can measure the local growth rate. Combining with $\sigma_{8,g} \simeq 0.80 \pm 0.05$ from PSCz catalogue[44], we have $f\sigma_8 = 0.403 \pm 0.031$. Figure 4 displays the evolution of $f\sigma_8(z)$ with respect to redshift z under Planck/ Λ CDM model[26] as well as the $f\sigma_8(z)$ data from various large-scale structure surveys. We see that our constraint with small error bar is very competitive with the other existing constraints. On the other hand, the cosmic accelerated expansion would be caused by the presence of a scalar field with an evolving equation of state, or extensions of general relativity[54, 55]. Although they produce similar expansion rates, different models predict measurable differences in the growth rate of structure[16, 56]. Future GWs from BNSs could be observed by ET[30] at a redshift of $z = 2$. The growth rates at different cosmic times can be measured by our method, which can determine the origins of the cosmic accelerated expansion.

From redshift space distortion constraints, the current matter density Ω_{m0} degenerates with $\sigma_{8,0}$ [57]. The precise peculiar velocities obtained directly from GWs at low redshifts can break this degeneracy. After correcting the Alcock-Paczynski (AP) effect[58] for the observed $f\sigma_8(z)_{\text{meas}}$, the parameters Ω_{m0} and $\sigma_{8,0}$ can be tightly constrained through

$$\chi^2 = \sum_{i=1} \frac{[f\sigma_8(\text{meas})_i - f\sigma_8(\text{model})_i]^2}{\sigma_i^2}. \quad (11)$$

The 1σ , 2σ and 3σ confidence contours in the Ω_{m0} - $\sigma_{8,0}$ parameter plane are shown in figure 5, where a flat Λ CDM model is assumed when calculating $f\sigma_8(z)_{\text{model}}$. The dashed contours show constraints from $f\sigma_8(z)$ at

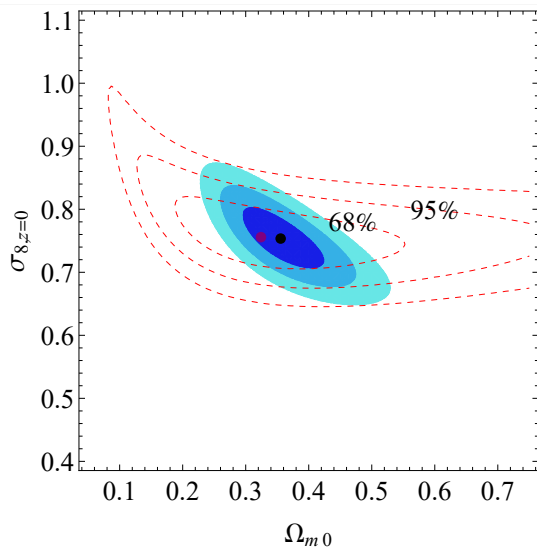


FIG. 5: Confidence contours of Ω_{m0} and $\sigma_{8,0}$ in Λ CDM model. The red dashed contours show the 1σ - 3σ confidence intervals using only high redshift ($z \geq 0.2$) $f\sigma_8$ measurements. The red point is the best fit. The blue contours show the same constraints for high redshift $f\sigma_8$ plus five low redshift data. The low-redshift $f\sigma_8$ can break the degeneracy between Ω_{m0} and $\sigma_{8,0}$. The best fit of Λ CDM model (black point) is $\Omega_{m0} \simeq 0.33 \pm 0.06$ and $\sigma_{8,0} \simeq 0.75 \pm 0.05$.

$z > 0.2$ in figure 5, while solid contours show the same constraints for the above data plus the peculiar velocity measurements from our method and other low-redshift $f\sigma_8$. We find that the best fit of Λ CDM model is $\Omega_{m0} \simeq 0.33 \pm 0.06$ and $\sigma_{8,0} \simeq 0.75 \pm 0.05$. After adding the low-redshift peculiar velocity measurements, the degeneracy can be broken.

Another serious problem called the H_0 tension[41] says that the Hubble constant estimated from the local distance ladder[25] is in 3.4σ tension with the value fitted from Planck CMB data assuming Λ CDM model[26]. From our simulation, the precise peculiar velocity measurements can constrain the Hubble constant with an uncertainty of 0.5%, which can reconcile the H_0 tension.

III. SUMMARY

The future GW detectors, such as ET[62], LISA[63], DECIGO[64] and BBO[65], will considerably enhance the angular resolution, distance measurement and the detection rate of GW events. More GW events will be detected and the host galaxies can be identified even without EM counterparts. The peculiar velocities measured by our method would be powerful cosmological tools. Although the method we propose may be limited by the reconstructed peculiar velocity field, future galaxy surveys, such as Euclid[66] and WFIRST[67], can give high-quality peculiar velocity field in the near future.

Acknowledgements

We thank the anonymous referee for useful comments and suggestions. We thank Enzo Branchini for providing the data of PSCz peculiar velocity field and critical reading the manuscript. This work is supported by the National Basic Research Program of China (973 Program, grant No. 2014CB845800), the National Natural Science Foundation of China (grants U1831207, 11422325 and 11373022), and the Excellent Youth Foundation of Jiangsu Province (BK20140016).

-
- [1] Abbott, B. P., et al., 2017, PRL, 119, 161101
 - [2] Abbott, B. P., et al., 2017, ApJL, 848, L12
 - [3] Goldstein, A., et al., 2017, ApJL, 848, L14
 - [4] Schutz, B. F., 1986, Nature, 323, 310
 - [5] Holz, D. E. & Hughes, S. A., 2005, ApJ, 629, 15
 - [6] Cutler, C. & Holz, D. E., 2009, PRD, 80, 104009
 - [7] Peebles P. J. E., 1993, Principles of Physical Cosmology. Princeton Univ. Press, Princeton, NJ
 - [8] Strauss, M. A., & Willick, J. A., 1995, Phys. Rep., 261, 271
 - [9] Abbott, B. P. et al. (KAGRA Collaboration, LIGO Scientific Collaboration and Virgo Collaboration), 2016, Living Rev. Relativity, 19, 1
 - [10] Hui, L., & Greene, P., 2006, PRD, 73, 123526
 - [11] Gordon, C., Land, K., & Slosar, A. 2007, PRL, 99, 081301
 - [12] Ben-Dayan, I., et al. 2014, PRL, 112, 221301
 - [13] Guzzo, L. et al., 2008, Nature, 451, 541
 - [14] Kaiser, N., 1987, MNRAS, 227, 1
 - [15] Zhang, P. J., Pan, J., & Zheng, Y. 2013, PRD, 87, 063526
 - [16] Huterer, D., Shafer, D. L., 2018, Rep. Prog. Phys. 81, 016901
 - [17] Riess, A. G., Davis, M., Baker, J., & Kirshner, R. P. 1997, ApJ, 488, L1
 - [18] Tully, R. B., & Fisher, J. R., 1977, A&A, 54, 661
 - [19] Theureau, G., Hanski, M. O., Coudreau, N., Hallet, N., & Martin, J. M., 2007, A&A, 465, 71
 - [20] Springob, C. M., et al., 2007, ApJS, 172, 599
 - [21] Djorgovski, S., & Davis M., 1987, ApJ, 313, 59
 - [22] Willick, J. A., Courteau, S., Faber, S. M., Burstein, D., Dekel, A., & Strauss M. A., 1997, ApJS, 109, 333
 - [23] Abbott, B. P., et al., 2017, Nature, 551, 85
 - [24] Levan, A. L., et al., 2017, ApJL, 848, L28
 - [25] Riess, A. G. et al., 2016, ApJ, 826, 56
 - [26] Planck Collaboration, Ade, P. A. R., Aghanim, N., et al. 2016, A&A, 594, A13
 - [27] Hjorth, J. et al., 2017, ApJL, 848, L31
 - [28] Springob, C. M., et al., 2014, MNRAS, 445, 2677
 - [29] Colless, M., Saglia, R. P., Burstein, D., Davies, R. L., McMahan, R. K., & Wegner, G., 2001, MNRAS, 321, 277
 - [30] Abernathy, M. et al. 2011, Einstein gravitational wave

- telescope: conceptual design study, European Gravitational Observatory, document number ET-0106C-10
- [31] Kawamura, S., Nakamura, T., Ando, M., et al. 2006, *Classical and Quantum Gravity*, 23, S125
 - [32] Liao, K., et al., 2017, *Nature Communications*, 8, 1148
 - [33] Branchini, E. et al., 1999, *MNRAS*, 308, 1
 - [34] Zhao, W., & Wen, L., 2018, *PRD*, 97, 064031
 - [35] Hinshaw, G., et al., 2009, *ApJS*, 180, 225
 - [36] Radburn-Smith D. J., Lucey J. R., Hudon M. J., 2004, *MNRAS*, 355, 1378
 - [37] Yahil A., Strauss M. A., Davis M., Huchra J. P., 1991, *ApJ*, 372, 380
 - [38] Foreman-Mackey D., Hogg D. W., Lang D., Goodman J., 2013, *PASP*, 125, 306
 - [39] Ma, Y.-Z., Branchini, E., & Scott, D., 2012, *MNRAS*, 425, 2880
 - [40] Hudson, M. J., & Turnbull, S. J., 2012, *ApJL*, 751, L30
 - [41] Freedman, W. L., 2017, *Nature Astronomy*, 1, 0121
 - [42] Macaulay, E., Wehus, I. K., Eriksen, H. K., 2013, *PRL*, 111, 161301
 - [43] Kazantzidis L. & Perivolaropoulos, L. 2018, *PRD*, 97, 103503
 - [44] Hamilton, A. J. S., & Tegmark, M., 2002, *MNRAS*, 330, 506
 - [45] Johnson, A. et al., 2014, *MNRAS*, 444, 3926
 - [46] Turnbull, S. J. et al., 2012, *MNRAS*, 420, 447
 - [47] Huterer, D. et al., 2017, *JCAP*, 05, 015
 - [48] Beutler, F. et al., 2012, *MNRAS*, 423, 3430
 - [49] Blake, C. et al., 2011, *MNRAS*, 415, 2876
 - [50] Song, Y. -S, & Percival, W. J. 2009, *JCAP*, 10, 004
 - [51] Satpathy, S., et al. 2017, *MNRAS*, 469, 1369
 - [52] de la Torre, S., et al., 2017, *A&A*, 608, A44
 - [53] Lewis, A., Challinor, A., & Lasenby, A., 2000, *ApJ*, 538, 473
 - [54] Dvali, G., Gabadadze, G. & Porrati, M., 2000, *PLB*, 485, 208
 - [55] Carroll, S. M., Duvvuri, V., Trodden, M. & Turner, M. S. 2004, *PRD*, 70, 043528
 - [56] Linder, E. V. 2005, *PRD*, 72, 043529
 - [57] Peacock, J. A. et al., 2001, *Nature*, 410, 169
 - [58] Alcock, C., & Paczynski, B. 1979, *Nature*, 281, 358
 - [59] Silveira V., & Waga I., 1994, *PhRvD*, 64, 4890
 - [60] Nesseris, S., Pantazis, G., & Perivolaropoulos, L. 2017, *PhRvD*, 96, 023542
 - [61] The eLISA Consortium. e-print (arXiv:1305.5720)
 - [62] "The Einstein Telescope Project", <https://www.et-gw.eu/et/>.
 - [63] "The Laser Interferometer Space Antenna", <https://www.lisamission.org/>
 - [64] "The Deci-Hertz Interferometer Gravitational wave Observatory", http://tamago.mtk.nao.ac.jp/decigo/index_E.html
 - [65] "The Big Bang Observer", <https://dx.doi.org/10.2514/6.2005-6711>
 - [66] "Euclid", <https://www.euclid-ec.org/>
 - [67] "Wide Field Infrared Survey Telescope", <https://wfirst.gsfc.nasa.gov/>